ORIGINAL PAPER

Aridity-driven divergence in soil microbial necromass carbon in alpine grasslands of the Tibetan Plateau

Yunfei Zhao[1,2] · Xia Wang[1] · Yazhen Li[1] · Menghan Yuan[1] · Jia Li[1] · Huawei Zhu[1] · Zhuoyun Cheng[1] · Wenhui Duan[1] · Junwu Wang[1]

Abstract

Soil microbial necromass carbon (MNC) contributes to the long-term stability of soil organic carbon (SOC). However, the response of MNC across aridity gradients remains unclear, especially in vulnerable alpine ecosystems. Here, we examined alpine grasslands from 180 sites spanning a 3,500 km aridity gradient on the Tibetan Plateau to investigate how MNC abundance and composition (contributions of bacterial and fungal necromass carbon) vary with climate. MNC was variable, ranging from 0.55 to 26.95 g kg^{-1} soil, with higher content observed in humid and dry-subhumid regions than in arid and semiarid regions in the Western Tibetan Plateau. Soil properties were the dominant drivers of MNC, with soil fertility (cation exchange capacity and total phosphorus) and weathering products (clay, silt and iron/aluminum oxides) facilitating MNC accumulation, while a negative correlation was observed between MNC and soil pH. A pivotal aridity threshold of 0.60 underpinned a non-linear decrease in MNC with increasing aridity across soil condition gradients; MNC was negatively correlated with aridity below this threshold and showed no correlation beyond it. Given this pivotal aridity threshold, we delineated the drivers of MNC under conditions of low (aridity < 0.6) versus high (aridity > 0.6) aridity. In low-aridity conditions, MNC accumulation was governed by aridity, soil fertility, weathering products, and pH, whereas in high-aridity conditions, the interplay between soil properties and temperature took precedence. Species richness enhanced carbon accumulation from microbial residues under low-aridity conditions more so than under high-aridity conditions, with fungal necromass carbon consistently being a higher contributor to SOC than bacterial necromass carbon, particularly in humid regions. These findings highlight aridity-driven divergence in MNC and propose that conserving plant diversity may mitigate the adverse effects of aridification on MNC under low-aridity conditions in alpine grasslands.

Keywords Tibetan Plateau · Alpine grassland · Aridity · Microbial necromass carbon · Biomarker · Soil organic carbon

Introduction

Soil organic carbon (SOC) is the largest active carbon reservoir in terrestrial ecosystems, with current stocks estimated at approximately 1500 Pg C, surpassing atmospheric and vegetation carbon (C) reservoirs (Hicks Pries et al. 2017; Friedlingstein et al. 2022).

✉ Xia Wang
wangxia@lzu.edu.cn

1 Gansu Key Laboratory for Environmental Pollution Prediction and Control, College of Earth and Environmental Sciences, Lanzhou University, Lanzhou 730000, China

2 Key Laboratory of Western China's Environmental Systems (Ministry of Education), College of Earth and Environmental Science, Lanzhou University, Lanzhou 730000, China

The storage and stability of SOC are determined by the balance between the production and decomposition of organic carbon, primarily derived from plants (litter, roots and secretions), and further supplemented by contributions from microorganisms (microbial residues and metabolites) (Liang et al. 2019; Terrer et al. 2021). While recalcitrant substances contribute to the long-term stability of SOC, more decomposable organic materials fuel microbial energy needs, facilitating the conversion into MNC through microbial synthesis and assimilation (Liang et al. 2017; Angst et al. 2021; Sokol et al. 2022). MNC comprises microbial cell membrane fragments and small microbial polymers, contributing to SOC sequestration (Craig et al. 2022; Ma et al. 2022; Xiao et al. 2023). In fact, MNC constitutes 30–60% of SOC in various ecosystems (e.g., grasslands and forests) and climatic zones (Wang et al. 2021a; Cao et al.

2023; Xue et al. 2023). Therefore, the mechanisms underlying microbial carbon accumulation must be elucidated to comprehensively understand SOC formation and stability.

MNC abundance is shaped by two interrelated processes: microbial carbon biomass production and MNC stability. The former is influenced by microbial growth and utilization efficiency while the latter is governed by physical and chemical protection mechanisms. Both processes are regulated by a combination of biotic and abiotic factors. In the soil microbial community, differences in fungal and bacterial cell composition contribute to variations in the accumulation and stability of their residues after death (Deveau et al. 2018; Li et al. 2022, 2024). Changes in litter quantity, resulting from shifts in vegetation composition and diversity along various environmental gradients, can influence the efficiency of MNC production (Jia et al. 2021; Spohn et al. 2023). Variations in climate and soil properties may indirectly influence the transfer and stability of microbial metabolites by affecting microbial physiological characteristics (Liang et al. 2017; Bahram et al. 2018; Hao et al. 2021; Wang et al. 2021b). Soil properties, including pH, total nitrogen and phosphorus, texture, and iron and aluminum oxides, critically influence microbial community activity, microbial growth rates, and the protective role of residual carbon, ultimately determining the persistence of MNC during the processing and stabilization of organic inputs in the soil (Hu et al. 2020; Bai and Cotrufo 2022; Bao et al. 2022; Qu et al. 2024).

Although climate predominantly influences the stability of MNC by regulating plant composition, microbial communities, and biogeochemical processes, a consensus on the response of MNC to climate change remains elusive. Some field experiments and large-scale surveys have found that increasing temperatures decrease the MNC content (Shao et al. 2018; Cao et al. 2023). Meanwhile, higher temperatures have also led to increased microbial biomass, favoring the accumulation of MNC in other reports (Ding et al. 2019; Angst et al. 2021). Furthermore, increases in precipitation can potentially increase (Wen et al. 2023; Xue et al. 2023), decrease (Chen et al. 2020), or exert no significant effect on MNC content (Hao et al. 2021; Wang et al. 2021a). Additionally, controlled experiments and observational studies have revealed inconsistent shifts in the proportion of fungal to bacterial necromass carbon in MNC (Xia et al. 2019; Wang et al. 2021a). The determinants of MNC and the magnitude and direction of their impacts depend on climatic conditions and biome types.

Grassland ecosystems cover approximately 40.5% of the Earth's land area and store approximately one-third of the global terrestrial carbon (White et al. 2000; Bai and Cotrufo 2022). MNC has been studied predominantly in temperate and tropical systems (Chen et al. 2020; Jia et al. 2021), with few studies focusing on alpine ecosystems, particularly the alpine grasslands that constitute more than 60% of the Tibetan Plateau, an area extremely sensitive and vulnerable to climate change (UNEP 2022). Although strong bifurcations in SOC, mineral-associated SOC, pH, and soil morphology have been observed at specific geographic and hydroclimatic boundaries (Slessarev et al. 2016; Kramer and Chadwick 2018; Heckman et al. 2023), the effects of the hydroclimatic threshold on the stability and composition of MNC remain unclear. Moreover, the Tibetan Plateau exhibits considerable variability in soil moisture, and although some experimental and regional studies have explored the mechanisms underlying MNC retention in the plateau (Ding et al. 2019; He et al. 2022), plateau-scale research is lacking. Particularly, the mechanisms driving the shifts in MNC under arid conditions remain unknown.

To address this knowledge gap, we conducted a 3500-km survey spanning a wide range of aridity in alpine grasslands across the Tibetan Plateau that examined vegetation characteristics, soil properties, and climate data and analyzed amino sugars as biomarkers. Amino sugars, which are commonly used as MNC biomarkers, including glucosamine(Gluc) primarily sourced from fungi and bacteria and muramic acid (Mura) exclusively from bacteria, were specifically employed to characterize the ratio of fungal to bacterial necromass carbon (Xia et al. 2019; Li et al. 2022). The main objectives of this study were (1) to investigate distribution patterns of MNC abundance and composition along aridity gradients and (2) to explore how climate, soil properties, and vegetation characteristics drive the variability of MNC with shifts in aridity. Two hypotheses guided this work: (1) MNC decreases with increasing aridity, exhibiting a distinct change at a specific aridity threshold, due to nonlinear reductions in carbon inputs and soil microbial biomass (Berdugo et al. 2020; Xu et al. 2020); (2) given that aridity affects MNC production, persistence, and interactions with soil properties and vegetation characteristics (Hao et al. 2021; Xue et al. 2023; Zhang et al. 2023), the primary drivers of MNC abundance vary across the aridity threshold.

Materials and methods

Study areas and field sampling

The Tibetan Plateau is characterized by a unique climate system owing to its geographical identity. Intense solar radiation, mean annual temperatures of approximately 1.7 °C with extremes reaching as low as -40 °C, and notable diurnal temperature variations define the region's climate. The precipitation distribution exhibits substantial spatial variability, with annual averages spanning 50–1000 mm and decreasing from northwest to southeast. The majority of rainfall occurs during the monsoon season from May to

September, accounting for approximately 90% of the total annual rainfall. The aridity index of the plateau displayed a marked gradient, placing most of the terrain within arid to semi-arid subarctic climatic zones. The landscape of the plateau comprises alpine steppes and meadows, with predominantly cold-tolerant and drought-resistant vegetation occupying more than 60% of the area. The dominant species in alpine grasslands are *Kobresia parva*, *Kobresia humili*, *Stipa purpurea*, and *Carex moorcroftii* (He et al. 2022; Zhao et al. 2023).

Fieldwork conducted in August over the years 2016–2021 included comprehensive soil and plant specimen collection along a 3500 km transect across the plateau. In total, 180 sites were sampled (97 sites from alpine steppes; 83 sites from meadows; with aridity ranging from 0.15 to 0.94) (Fig. 1a). A large quadrat (30 × 30 m) was established at each site, within which three 1 m × 1 m subquadrats were defined to replicate vegetation and soil sampling. The plant species composition was documented in each subquadrat, and species counts across the three were aggregated to provide a site-wide species abundance metric. A zero-level cut within each subquadrat was used to sample the aboveground plant biomass. Concurrently, soil samples were uniformly collected from a standardized 10 cm depth across all subquadrats, with each subsequently undergoing rigorous laboratory analysis.

Analysis of soil physicochemical properties

Soil samples were air-dried indoors, after which rocks and roots were removed. The soil was then ground to analyze its physicochemical properties. SOC content was determined using a Primacs ATC100 analyzer (Skalar, Netherlands) after removing inorganic carbon. Soil pH was measured using a pH electrode (1:2.5 soil: distilled water ratio). Total nitrogen (TN) was quantified through the automatic Kjeldahl distillation method. Total phosphorus (TP) was determined using a colorimetric method following digestion with hydrofluoric and perchloric acids (Lu 1999). Soil particle size was assessed using a laser grain-size analyzer (Masterizer 2000; Malvern Panalytical, Malvern, UK). Cation exchange capacity (CEC) was measured via the cobalt hexamine chloride method (Aran et al. 2008), and soil electrical conductivity (EC) was determined using a conductivity meter. Soil iron and aluminum oxides were extracted using a solvent (Lalonde et al. 2012) and quantified using ICP-OES (iCAP 7400; Thermo Fisher Scientific, Waltham, MA, USA). Free Fe/Al oxide ($Fe_d + Al_d$) content was evaluated using the citrate-bicarbonate-dithionite method, amorphous Fe/Al oxide ($Fe_o + Al_o$) content using an oxalic acid-ammonium oxalate buffer (pH 3.2 with ammonia), and complexed Fe/Al oxide ($Fe_p + Al_p$) content with a sodium pyrophosphate solution.
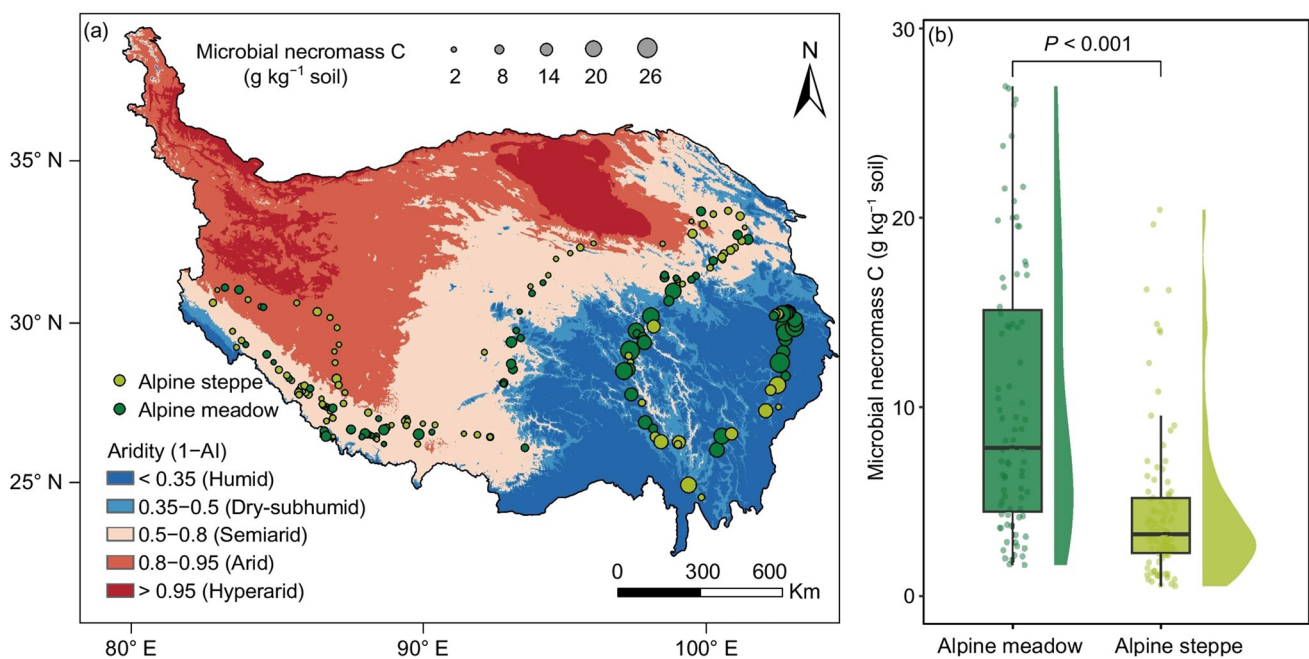

Fig. 1 Distribution pattern of microbial necromass carbon across alpine grasslands on the Tibetan Plateau. (**a**) Spatial distribution of microbial necromass carbon in alpine grasslands, with bubble size proportional to the corresponding variable value. Larger bubbles represent higher values. (**b**) Raincloud plot and boxplot distribution of microbial necromass carbon in different grassland types. The boxplot center represents the median, and the box limits define the interquartile range. Raincloud plots show probability density

Analysis of amino sugars for soil MNC

Soil amino sugars were determined using the acid hydrolysis method (Zhang and Amelung 1996), which measures Gluc, Mura, galactosamine, and mannosamine. The specific procedure was as follows: a soil sample (1.0 g) was weighed and transferred to a 50 mL hydrolysis flask, to which 10 mL of 6 M HCl was added, and the mixture was hydrolyzed at 105 °C for 8 h. The mixture was cooled to room temperature, and 100 μL of inositol was added. The resultant liquefied sample underwent filtration and was then subjected to rotary evaporation at 52 °C. Dissolution of the remaining solids in ultrapure water and adjustment of the solution's pH to a neutral range between 6.6 and 6.8 with 1 M KOH preceded the centrifugation step at $1000 \times g$ for 10 min. The supernatant was evaporated and dissolved in methanol. After centrifugation at $1000 \times g$, the liquid was transferred to a specialized derivation vial and evaporated under a nitrogen atmosphere at a moderate 45 °C. Ultrapure water and N-methylglucamine were added to the residue before the sample was lyophilized. The subsequent derivatization phase involved a treatment with hydroxylamine hydrochloride and 4-dimethylaminopyridine agitated and heated for half an hour within a temperature range conducive to chemical reaction (75–80 °C). Acetic anhydride and dichloromethane were used in further modification steps, ensuring the reaction completeness and removal of the hydrophilic phase. Following an additional careful phase-separation with ultrapure water, the organic extract was dried under nitrogen, then combined with an ethyl acetate and n-hexane mixture, and finally presented for compositional analysis via the Trace 1300 gas chromatograph (Thermo Fisher Scientific) equipped with a TG-1MS (30 m $\times$ 0.25 mm $\times$ 0.25 μm) capillary column and flame ionization detector. MNC and fungal and bacterial necromasses were calculated using equations derived from Liang et al. (2019):

$$Fungal\ necromass\ C = (Gluc/179.17 - 2 \times Mura/251.23) \\ \times 179.17 \times 9 \tag{1}$$

$$Bacterial\ necromass\ C = Mura \times 45 \tag{2}$$

$$MNC = Fungal\ necromass\ C + Bacterial\ necromass\ C \tag{3}$$

where 179.17 and 251.23 are the molecular weight of Gluc and Mura, respectively; 9 represents the conversion factor of Gluc to fungal necromass C; and 45 is the conversion factor of Mura to bacterial necromass C (Appuhn and Joergensen 2006; Joergensen 2018). Fungal necromass C was calculated by subtracting the bacterial Gluc from total Gluc, with the assumption that Mura and Gluc occur at a 1:2 M ratio in bacterial cells (Engelking et al. 2007; Joergensen 2018). It should be noted that the estimation of MNC using amino sugars analysis has limitations and uncertainties, as it relies on conversion factors for extrapolation based on certain assumptions (Liang et al. 2019; Whalen et al. 2022).

Statistical analyses

All statistical analyses were conducted using R version 4.2.3 (R Core Team 2023). The normality of the data was assessed using the Shapiro–Wilk test. To compare differences in the data, a one-way analysis of variance was employed for normally distributed and homoscedastic data, and the Kruskal–Wallis non-parametric test was used for non-normally distributed data. Differences in MNC between alpine meadow and alpine steppe were analyzed using Kruskal–Wallis non-parametric test.

Boosted regression tree (BRT) analysis, rooted in the classification and regression tree algorithm, addresses the intricate non-linear interdependencies present within a dataset (Elith et al. 2008). This technique incorporates the process of stochastic sampling of data subsets during analytical computations, enhancing the capability to discern the relative importance of explanatory variables affecting the outcome variable, namely MNC. The ideal tree count for BRT was determined using tenfold cross-validation, assessing model accuracy with cross-validated root mean squared error (RMSE) and R^2 (Table S1).

Linear multiple regression was employed to investigate the unique and shared effects of the three major mechanisms on MNC variance partitioning, providing coefficient values that illustrate the directional influence of each variable. The predictor variables aligned with those used in the linear multiple regression and were categorized into (1) climate factors, including aridity, defined as $1 -$ aridity index, with the aridity index calculated as the ratio of annual precipitation to potential evapotranspiration; mean annual temperature; precipitation seasonality, the coefficient of variation of monthly precipitation; and temperature seasonality, the standard deviation of monthly mean temperatures, (2) vegetation characteristics including aboveground biomass and species richness, and (3) soil properties including $Fe_p + Al_p$, $Fe_o + Al_o$, $Fe_d + Al_d$, soil silt, clay, soil pH, soil C/N, EC, CEC, soil total potassium (TK), and total phosphorus (TP).

We performed simple linear and non-linear regressions and a threshold regression model to evaluate how MNC responded to increasing aridity. Among these, the threshold model exhibited the lowest Akaike Information Criterion value, indicating a superior fit compared to the simple linear and non-linear regressions (Table S2). Thresholds were identified using threshold models (e.g., segmented or segmented regressions) from the "chngpt" R package (Berdugo et al. 2020) and validated through bootstrapped

regressions and the Kruskal–Wallis test. Subsequently, the sites were categorized into low (< 0.6, n = 72) and high (aridity > 0.6, n = 108) aridity levels based on the thresholds.

Mantel tests were conducted to analyze the impact of environmental factors on MNC composition (including fungal and bacterial necromass carbon) in less (aridity < 0.6) and more (aridity > 0.6) arid sites. To further quantify the individual impacts of each environmental variable on the variance in MNC composition within the aridity categories and across the entire dataset, hierarchical partitioning was performed using the R package "rdacca.hp" (Lai et al. 2022).

We further used the "piecewiseSEM" R package to construct segmented structural equation models (PSEM) under two aridity levels and investigate the direct and indirect relationships between MNC and soil properties, vegetation characteristics, and climate. The environmental factors driving MNC at low and high aridity levels were categorized as aridity, mean annual temperature, soil weathering products ($Fe_p + Al_p$, $Fe_o + Al_o$, $Fe_d + Al_d$, soil silt, and clay), soil fertility (CEC and TP), soil pH, and vegetation characteristics (aboveground biomass and species richness). Principal component analysis (PCA) was employed to decrease the multitude of variables. The reliability of PCA results was assessed using Kaiser–Meyer–Olkin (KMO) and Bartlett's sphericity tests (BS), ensuring KMO ≥ 0.5 and BS < 0.001 (Table S3 and S4). A structural equation model established based on prior knowledge showed that climatic variables (mean annual temperature and aridity) drive variations in other environmental factors, while vegetation characteristics, weathering products, soil fertility, and pH directly influence MNC by regulating carbon input and MNC formation and preservation. In the segmented SEM modeling process, paths with the smallest p-values (< 0.05) were integrated into the model through directed separation and were iteratively refined until a satisfactory fit was achieved. The decision to include a missing path was guided by the theoretical relationships between the variables in that path. The optimal model was constructed using Fisher's C-test and AIC comparisons (Grace 2006; Shipley 2016).

Results

Changes in MNC with aridity gradients on the Tibetan Plateau

Soil MNC exhibited considerable variation across the 180 alpine grassland sampling sites on the Tibetan Plateau (Fig. 1a). Specifically, MNC ranged between 0.55 and 26.95 g kg^{-1} soil, with an average of 7.20 ± 0.48 g kg^{-1} soil. Higher aridity corresponded to a lower MNC in the western Tibetan Plateau. Notably, MNC was significantly higher ($P < 0.001$) in the alpine meadow (10.30 ± 0.79 g kg^{-1}

soil) than in the alpine steppe (4.54 ± 0.41 g kg^{-1} soil) (Fig. 1b). The composition of MNC varied between arid and dry-subhumid regions, with the lowest ratio of fungal to bacterial necromass carbon occurring in arid regions (3.50 ± 0.31, Fig. 2a). MNC content was significantly higher in humid (15.14 ± 1.21 g kg^{-1} soil) and dry-subhumid (12.03 ± 1.33 g kg^{-1} soil) regions than in arid (3.38 ± 0.48 g kg^{-1} soil) and semiarid (4.59 ± 0.34 g kg^{-1} soil) regions. The contribution of fungal necromass carbon to SOC was lower in arid regions ($23.46 \pm 1.98\%$) than in other regions (Fig. 2b). The contribution of fungal necromass carbon to SOC ($27.87 \pm 0.80\%$) surpassed that of bacterial necromass carbon ($7.39 \pm 0.27\%$) across all climate zones (Fig. 2b).

Determinants of MNC across alpine grasslands on the Tibetan Plateau

To identify the factors influencing MNC distribution patterns, we focused on four climatic variables (aridity, mean annual temperature, precipitation seasonality and temperature seasonality), two vegetation variables (aboveground biomass and species richness), and eleven soil variables ($Fe_p + Al_p$, $Fe_o + Al_o$, $Fe_d + Al_d$, silt, clay content, pH, C/N, EC, CEC, TK, and TP). The BRT analysis established a predictive model combining climate, vegetation, and soil variables that outperformed individual factors in predicting MNC (Table S1). The highest CV-R^2 (0.78) and lowest CV-RMSE (0.46) were achieved when the model incorporated all variables (vegetation, climate and soil properties). The relative importance of each variable in the comprehensive model is shown in Fig. 3a. Soil properties accounted for the majority of explanatory variance in MNC (70.29%), whereas climate and vegetation accounted for 19.89% and 9.82%, respectively (Fig. 3a). Among the individual variables, $Fe_p + Al_p$ (18.90%) exhibited the greatest influence on MNC, followed by CEC (17.27%), aridity (13.42%), pH (10.06%), TP (8.04%), aboveground biomass (7.22%), and silt (4.39%) (Fig. 3a). Partial dependence plots visually illustrate the impact of environmental variables on the distribution of MNC (Fig. S1).

Multiple regression analysis, including both biotic and abiotic variables, such as climate, vegetation characteristics, and soil properties, explained 79% of the spatial variation in the MNC. In line with the BRT analysis, multiple regression analysis indicated that soil properties accounted for 70% of the total variance in MNC (Fig. 2b). Among the various edaphic variables examined, $Fe_p + Al_p$, CEC, pH, and TP emerged as important factors explaining the spatial variation in MNC (Fig. 3b). The vegetation-related effects were weak and were mainly represented by aboveground biomass and species richness (R^2 = 0.08, Fig. 3b), which were positively correlated with MNC (Fig. 3b). Climatic factors, although
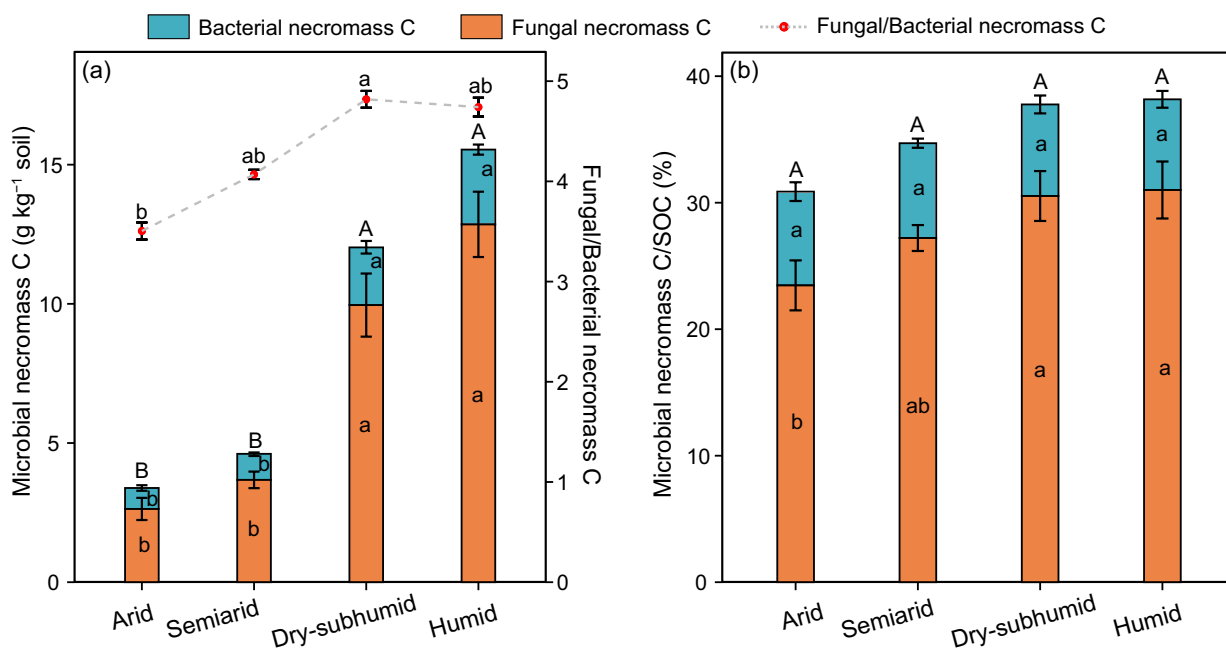
Fig. 2 Soil microbial necromass carbon and ratio of fungal to bacterial necromass carbon. Microbial necromass carbon (**a**) and its contribution to SOC (**b**) in different climate zones. Error bars denote standard errors of the means. Significant differences in fungal and bacterial necromass carbon and total microbial necromass carbon among climate zones are indicated by lowercase and uppercase letters, respectively, at $P < 0.05$

less influential than soil properties, still played a considerable role, accounted for 16% of the MNC variance (Fig. 3b); the strongest contribution was from aridity (Fig. 3b), with MNC decreasing as aridity increased (Fig. 3b).

Drivers of soil MNC at low and high aridity levels

The association between MNC and aridity was modeled using linear or generalized additive models (Fig. 4 and Table S2). The MNC–aridity relationship was best captured by the generalized additive model, as indicated by the AIC (Fig. 4a; $R^2 = 0.50$). MNC demonstrated a non-linear decrease as aridity increased. Threshold regression analysis revealed associations between the aridity threshold and MNC. This threshold-like behavior was consistent with the observations in the partial dependence plots (Fig. S1). Specifically, MNC sharply decreased with drought below the threshold of 0.60; however, beyond this threshold, the relationship between MNC and aridity weakened and gradually leveled off (i.e., with a lower slope) (Fig. 4 and Fig. S2).

Due to the shift in the MNC–aridity correlation occurring at the aridity threshold of 0.60, we categorized all sites into two groups: those with aridity levels <0.60 and >0.60, denoted low and high aridity levels, respectively, to assess the drivers of MNC content and composition (Figs. 5, 6 and S2). Employing the Mantel test, we explored the associations between environmental factors (climate, vegetation, and soil variables)

and MNC composition (contributions of bacterial and fungal necromass carbon) at sites with low (<0.6) and high (>0.6) aridity (Fig. 5a). For low aridity levels, the Mantel test revealed significant correlations between MNC composition and various factors, such as aridity, precipitation seasonality, CEC, TP, pH, TK C/N, clay, silt, and Fe/Al oxides ($P < 0.05$; Fig. 5a). In contrast, at high aridity levels, the MNC composition was significantly related to aboveground biomass, aridity, temperature seasonality, CEC, TP, clay, silt, and $Fe_p + Al_p$ ($P < 0.05$; Fig. 5a). Notably, mean annual temperature did not significantly affect MNC composition (Fig. 5a). Regardless of aridity levels, soil Fe/Al oxides, CEC, soil texture, and pH were the most influential factors shaping MNC composition (Fig. 5b). Aridity is an important factor affecting the distribution of MNC composition at low aridity levels, but not at high aridity levels. Moreover, silt loam and silt clay loam soils exhibited higher MNC levels and a greater fungal-to-bacterial necromass carbon ratio, whereas sandy and sandy loam soils showed lower values (Fig. S3). In summary, soil clay, iron/aluminum oxides, CEC and TP appear to be the dominant factors contributing to variations in MNC composition.

In addition, we unraveled the direct and indirect connections between climate, vegetation, soil weathering products (clay, silt and iron/aluminum oxide), soil fertility (CEC and TP), soil pH, and MNC using PSEM analysis (Fig. 6). This analysis revealed distinct key paths mediating these relationships at both low and high aridity
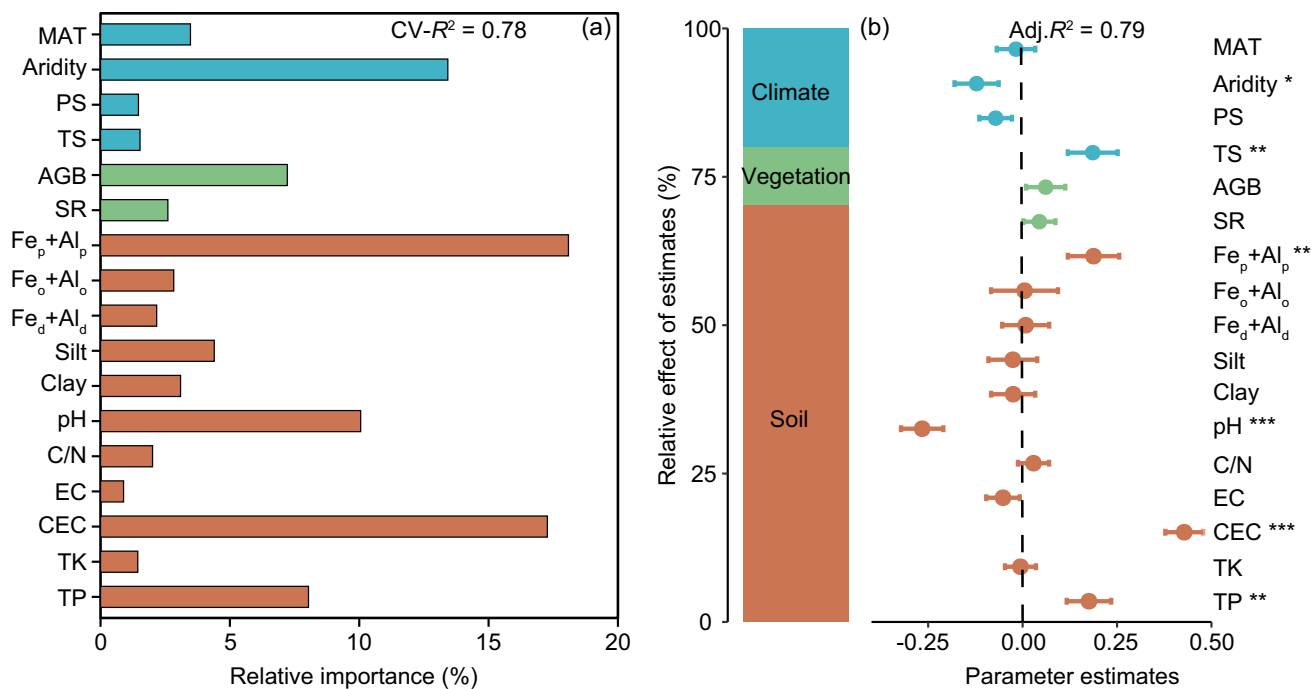
Fig. 3 Relative importance (%) of variables for the boosted regression tree model of soil microbial necromass carbon (**a**) and effects of each predictor on soil microbial necromass carbon (**b**) across alpine grasslands (n = 180). The average parameter estimates of model parameters (standardized regression coefficients) are displayed with their corresponding 95% confidence intervals and the relative importance of each predictor. The adjusted (adj.) R^2 of the model and the P value of each are: *$P < 0.05$; **$P < 0.01$; ***$P < 0.001$. Climate variables include aridity, mean annual temperature (MAT), Precipitation Sea-

sonality (PS), and Temperature Seasonality (TS); vegetation characters include aboveground biomass (AGB) and species richness (SR); soil properties include complexed Fe/Al oxides ($Fe_p + Al_p$), amorphous Fe/Al oxides ($Fe_o + Al_o$), free Fe/Al oxides ($Fe_d + Al_d$), soil silt, clay content, soil pH (pH), soil carbon and nitrogen ratio (C/N), electrical conductivity (EC), soil cation exchange capacity (CEC), total potassium (TK), and total phosphorus (TP)
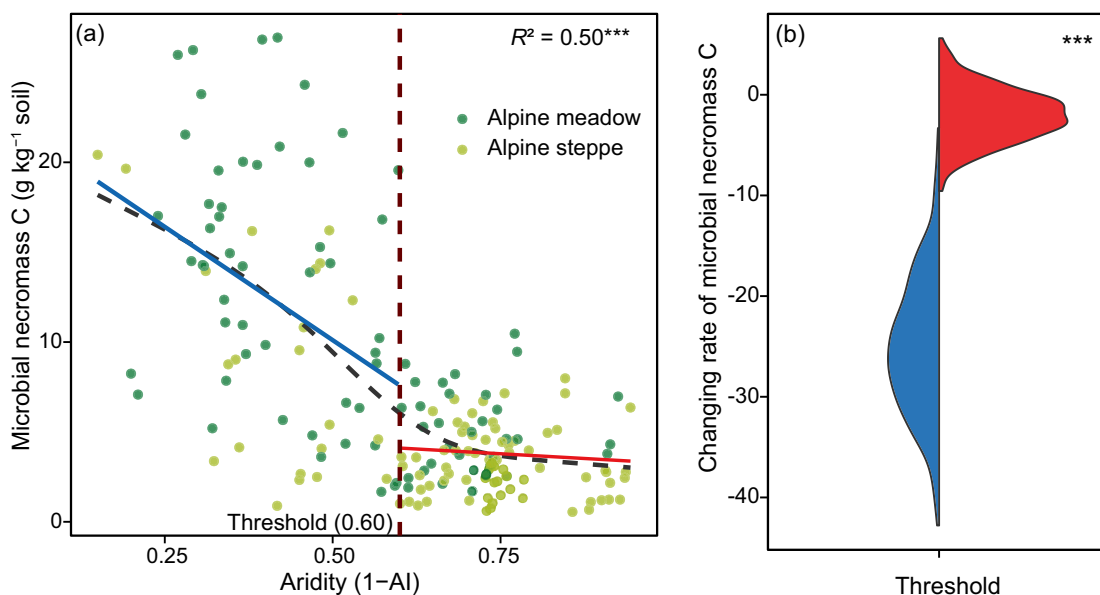

Fig. 4 Relationship between soil microbial necromass carbon and aridity. The black line represents the results for the entire alpine grassland generated using non-linear regression; vertical dashed lines

and inset text show the aridity thresholds identified (**a**). Violin plots depict the differences in bootstrapped slopes between the two regressions existing on each side of the threshold (**b**)
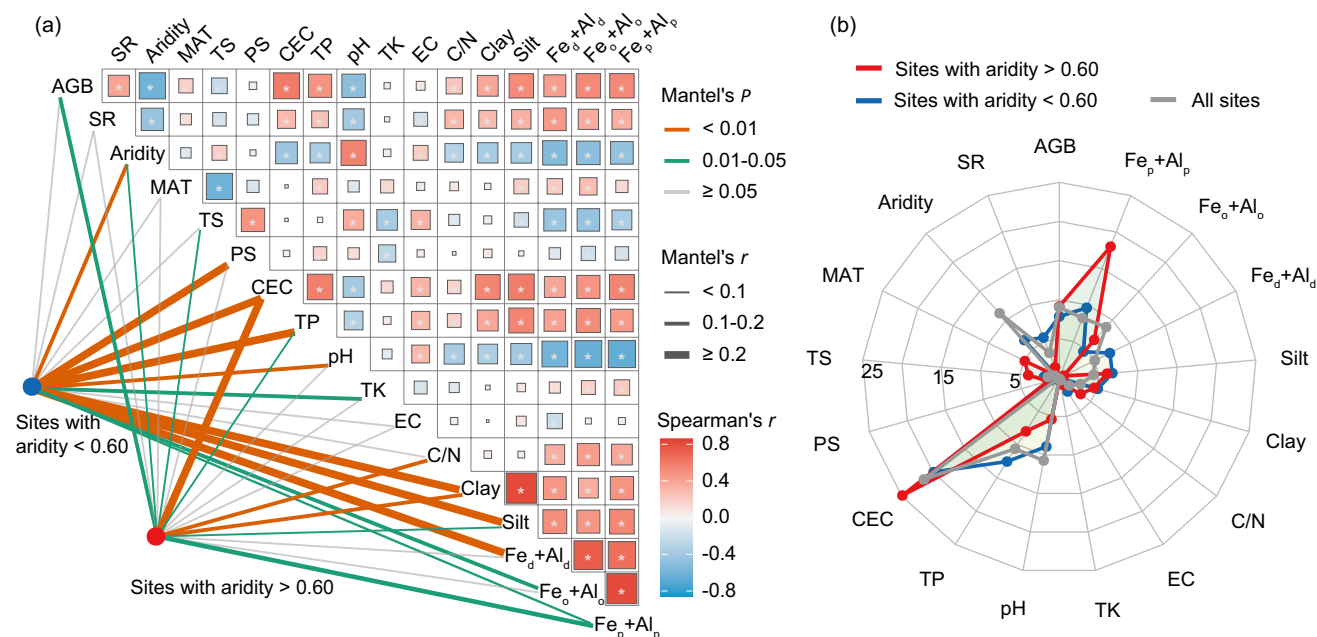
Fig. 5 Mantel test between soil microbial necromass carbon composition (soil fungal and bacterial necromass C) and environmental factors (**a**), and the contribution of individual factors to microbial necromass carbon composition (**b**) for sites with aridity < 0.6 (n = 72) and > 0.6 (n = 108). The thickness of the line represents the correlation coefficient (Mantel's r) and is scaled accordingly. The color gradient indicates the Spearman's correlation coefficients between variables. The width of the edges represents the Mantel's r value, and the color of the line denotes the significance of the differ-ences. Relative importance of environmental variables to soil fungal and bacterial necromass carbon for different aridity gradient zones. MAT, mean annual temperature; PS, precipitation seasonality; TS, temperature seasonality; AGB, aboveground biomass; SR, species richness; $Fe_p + Al_p$, complexed Fe/Al oxides; $Fe_o + Al_o$, amorphous Fe/Al oxides; $Fe_d + Al_d$, free Fe/Al oxides; C/N, soil carbon to nitrogen ratio; EC, electrical conductivity; CEC, soil cation exchange capacity; TK, total potassium; TP, total phosphorus

levels. At low-aridity sites, greater aridity significantly decreased soil mineral protection, soil fertility, aboveground biomass, and species richness, while increasing soil pH. Soil fertility proved to be the direct primary driver of MNC (path coefficient = 0.54) and was positively correlated with weathering products (path coefficient = 0.61) (Fig. 6a), which were not related to MNC. Conversely, at high-aridity sites, only vegetation characteristics were negatively associated with aridity (Fig. 6b). In low-aridity environments, aridity appeared to indirectly counteract the stabilizing roles of soil mineral protection and soil fertility. This was evident through a robust negative link between aridity and weathering products (path coefficient = −0.21). In addition, aridity indirectly diminished MNC by reducing productivity and species richness, lowering soil fertility, and impeding organic carbon accumulation (Fig. 6a). Alternatively, by increasing soil pH, aridity indirectly decreased MNC, as we observed a negative relationship between soil pH and MNC (path coefficient = −0.31) (Fig. 6a).

We observed MNC variation for sites with low and high aridity levels as follows: (i) at low-aridity sites, aridity, soil properties, and vegetation characteristics were important; increasing aboveground biomass and species richness and decreasing aridity contributed to higher MNC and complex influences on soil properties. The effects of mean annual temperature on MNC were complex and involved both direct and indirect effects. For instance, despite its direct positive linkage to MNC, mean annual temperature had a negligible net negative role on MNC (Fig. 6c). (ii) At high aridity sites, the interplay between soil mineral protection and soil fertility was crucial, along with the effects of mean annual temperature and soil pH, while the net effects derived from aridity were relatively limited (Fig. 6d).

Discussion

Distribution patterns of MNC in grasslands

The conspicuous reduction in MNC in the more arid regions of the Western Tibetan Plateau underscores the negative influence of climate, particularly aridity, on MNC and, therefore, SOC reserves. This pattern aligns with established paradigms that arid environments tend to support lower microbial biomass and activity owing to constraints on water availability and biological processes (Berdugo et al. 2020; Liu et al. 2023; Zhang et al. 2023). The MNC content was
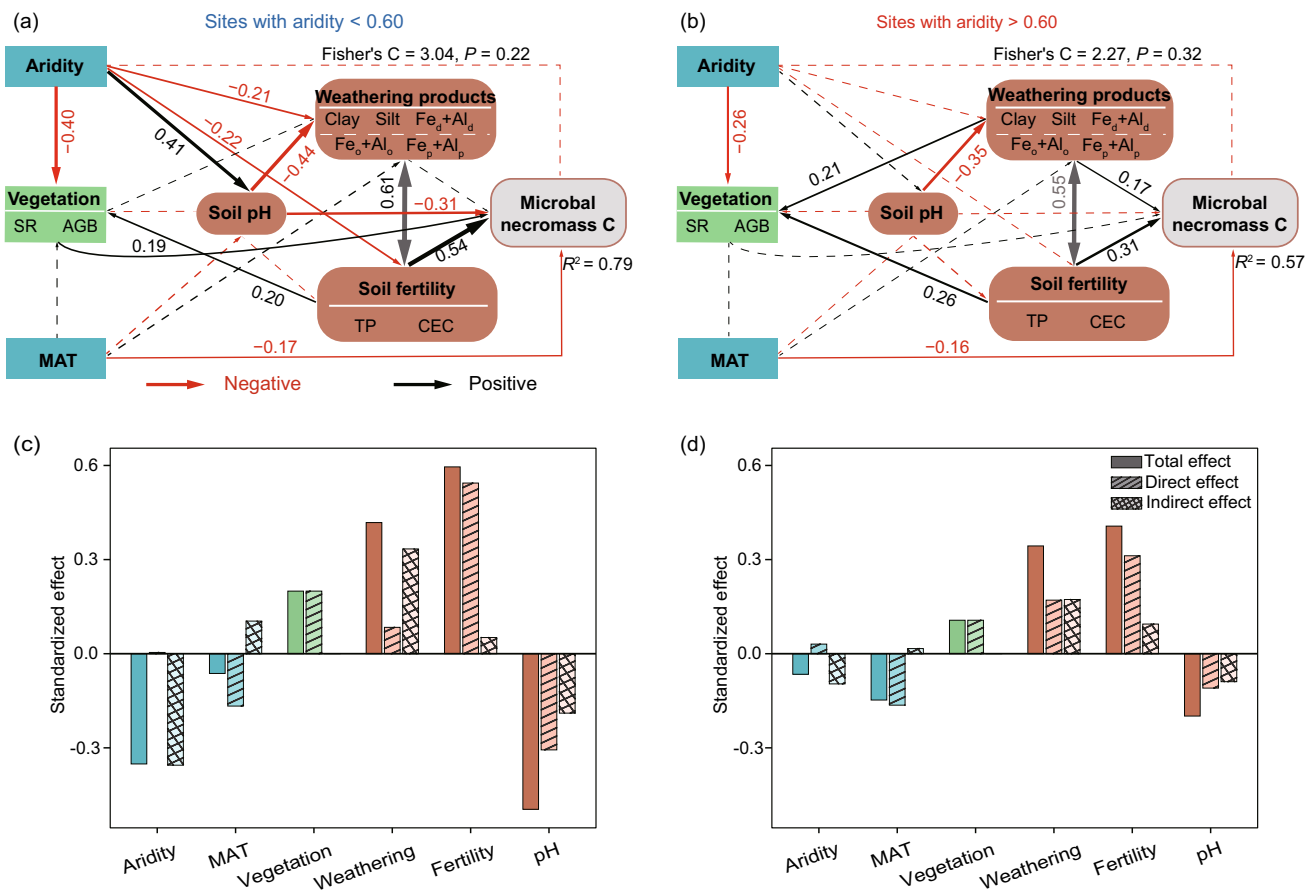
Fig. 6 Path diagram for piecewise structural equation modeling showing direct and indirect effects of environmental variables on microbial necromass carbon in sites with low (**a**; aridity < 0.6) and high (**b**; aridity > 0.6) aridity levels. Values next to arrows represent standardized effect sizes, and arrow thickness is scaled according to the magnitude of the effect size. Red arrows indicate a significant negative ($P < 0.05$) effect; black indicates a significant positive effect. Dashed arrows indicate non-significant relationships. Double-headed arrows between weathering products and soil fertility represent cor-

related terms. PCA using variables listed in rectangles identified vegetation characteristics, soil fertility, and weathering products as the first components. The standardized effects from structural equation modeling for sites with low (**c**) and high (**d**) aridity levels. MAT, mean annual temperature; AGB, aboveground biomass; SR, species richness; $Fe_p + Al_p$, complexed Fe/Al oxides; $Fe_o + Al_o$, amorphous Fe/Al oxides; $Fe_d + Al_d$, free Fe/Al oxides; CEC, cation exchange capacity; TP, total phosphorus

notably higher in humid and dry sub-humid regions than in arid and semiarid regions (Fig. 2a), which is consistent with global grassland patterns (Xue et al. 2023). The contribution of MNC to SOC in the alpine grasslands of the Tibetan Plateau (35%) was lower than that in grasslands globally (47%) (Wang et al. 2021a).

The ratio of fungal to bacterial necromass carbon in alpine grasslands (4.2; Fig. 2a) was significantly higher than the global grassland ratio of 2.5 (Wang et al. 2021a), indicating that fungal necromass carbon contributes more substantially to SOC in alpine grasslands compared to global grasslands. Generally, the fungal biomass in grasslands is much greater than the bacterial biomass, and ecosystems with higher microbial biomass tend to have more MNC (He et al. 2020; Li et al. 2022; Yang et al. 2022).

Furthermore, low temperatures and aridity can increase the fungal-to-bacterial biomass ratio, potentially due to the greater tolerance to nutrient and water scarcity generally exhibited by fungi compared to bacteria (Bahram et al. 2018). The ratio of fungal-to-bacterial necromass carbon and SOC content showed a significant positive correlation (Fig. S4). Fungal necromass carbon is more prone to mineral adsorption or restriction of its decomposition through association with aggregates (Six et al. 2006; Veloso et al. 2020; Xu et al. 2022). Based on comparative trends, the proportion of fungal-derived necromass carbon in alpine grassland soils under arid and cold conditions was greater than that in global grasslands; however, further empirical validation of these results are required.

Driving factors of MNC across alpine grasslands on the Tibetan Plateau

BRT and multiple regression analyses accentuated the multidimensionality of the factors influencing the MNC, with soil properties as the primary driving force. MNC showed a significant positive correlation with CEC, soil clay, and iron-aluminum oxides (Figs. 3b and S2). Abundant nutrients stimulate the growth and reproduction of microorganisms, leading to a faster microbial biomass turnover rate and increased MNC (Bahram et al. 2018; Prommer et al. 2020). The increase in soil iron-aluminum oxides and clay promotes MNC accumulation mainly because of the cohesive force of clay particles and the cementing effect of iron-aluminum oxides, which are conducive to the formation and stability of soil aggregates and weaken MNC decomposition through physical protection (Wiesmeier et al. 2019; Zhao et al. 2021; Xiao et al. 2023). In addition, soil iron and aluminum oxides interact with organic matter molecules through adsorption and co-precipitation processes, forming stable organo-mineral complexes that enhance the protection of MNC against decomposition (Wagai et al. 2020; Jeewani et al. 2021; Bao et al. 2022).

The MNC content decreased with increasing soil pH on the Tibetan Plateau, which is consistent with the negative correlation reported between MNC and pH in global ecosystems (Wang et al. 2021a). This may be because low pH values, typically ranging from 4.5 to 7, are preferred for fungal growth, thereby increasing fungal biomass and promoting the accumulation of MNC (Rousk et al. 2009; Hu et al. 2020). Soil pH also affects the physical protection of minerals. For example, soils with lower pH values (4.5 to 6.5) generally have a higher degree of weathering, and iron and aluminum oxides are more abundant, with stronger binding of carboxyl groups to mineral surfaces, thereby promoting MNC accumulation (Chen et al. 2021; Koester et al. 2021).

Although vegetation characteristics, such as aboveground biomass and species richness, have weaker influences on MNC, they still contribute to soil carbon inputs and offer substrates for MNC (Sokol et al. 2022). Species richness promoted the accumulation of MNC in alpine grasslands, a finding similar to that reported in subtropical forests (Jia et al. 2021). This may be attributed to increased species richness enhancing carbon inputs and root exudate secretion, as well as promoting microbial growth and biomass, collectively leading to MNC accumulation (Lange et al. 2015; Mellado-Vázquez et al. 2016; Prommer et al. 2020; Luo et al. 2021).

Aridity showed a strong negative correlation with MNC, whereas no correlation was detected between mean annual temperature and MNC (Figs. 3b and S2). This aligns with the results indicating that the accumulation of MNC in arid grasslands is mainly controlled by aridity (Ma et al. 2018). Additionally, a five-year warming and controlled water addition experiment in semi-arid grasslands indicated that increased precipitation favors MNC accumulation (Shao et al. 2018). The biomass of Tibetan Plateau grasslands is mainly limited by water availability, and a reduction in moisture weakens grassland productivity, hindering MNC accumulation (Zhang et al. 2021; Zhao et al. 2022). The MNC content in the alpine meadows was higher than that in the alpine steppes (Fig. 1b), further indicating that moist environmental conditions favor the accumulation of MNC.

Distinct mechanisms of soil MNC accumulation at low and high aridity levels

The application of generalized additive models and threshold regression revealed the non-linear response of MNC to increasing aridity, contingent upon an aridity threshold of 0.60 (Fig. 4). MNC may be relatively more resilient or adaptive to aridity to a certain point, which is consistent with studies that have reported threshold responses in ecosystem functions under environmental stress (Kramer and Chadwick 2018; Berdugo et al. 2020; Zhao et al. 2023). Below this threshold, aridity markedly reduced the MNC content, suggesting that in relatively less arid environments, water stress may swiftly curtail microbial biomass and necromass (Hao et al. 2021; Heckman et al. 2023; Zhang et al. 2023). These mechanisms may be linked to microbial community adaptation or alternative stabilization processes (Angst et al. 2021; Wang et al. 2021a; Sokol et al. 2022). In relatively wetter soils, elevated moisture levels may facilitate the enhanced interaction of inputs with mineral surfaces and promote the release of mineral and nutrient elements, resulting in increased MNC (Angst et al. 2021; Zhao et al. 2022; Heckman et al. 2023). The relative roles of drought and temperature in MNC accumulation differ across various ecosystem types (Hao et al. 2021; Wang et al. 2021a; Ma et al. 2022), which aligns with our finding that MNC in different arid regions exhibited distinct responses to aridity and mean annual temperature. Under relatively wetter conditions, aridity acts as a key determinant in controlling MNC abundance, whereas in arid regions, the impact of temperature on MNC is heightened.

The variability observed in species richness implies that its contribution to the MNC may fluctuate along the aridity gradient. Species richness under relatively wetter conditions significantly surpassed that in arid areas (Table S5). Furthermore, the link between species richness and MNC was more pronounced under relatively wet conditions than in arid areas (Fig. S2). This pattern may be attributed to moisture constraints on carbon input in arid soils, where the association between species richness and ecosystem productivity is weaker than that in relatively wet

soils (Grace et al. 2016; Zhao et al. 2022). Higher carbon input levels may also sustain a larger reservoir of mineral-associated soil carbon, potentially through the "microbial carbon pump" mechanism, wherein labile inputs increase microbial biomass production in humid soils (Liang et al. 2017; Heckman et al. 2023). Our results confirm that the relationship between MNC and species richness is modulated by climate, with the accumulation effects of species richness on MNC being stronger in the relatively wetter regions of the Tibetan Plateau.

Relatively wetter and arid soils exhibited divergence in the importance of soil properties related to variations in MNC content (Fig. 6). More specifically, soil weathering products (soil clay and iron/aluminum oxides) were strongly correlated with the increasing abundance of MNC in relatively wetter soils, but showed a weaker association in arid soils. These trends align with the emerging paradigm of iron/aluminum oxide effects on mineral-associated SOC and arid soils enriched with divalent alkaline cations, with cation bridging occurring between mineral surfaces and organic matter (Heckman et al. 2023). This may be attributed to the increased availability and transport of moisture in relatively wetter soils, increasing weathering rates which yields secondary iron and aluminum phases of varying crystallinity and clay minerals. This ultimately enhances MNC stability through complexation/co-precipitation and adsorption (Kramer and Chadwick 2018; Rasmussen et al. 2018; Huang et al. 2021; Bao et al. 2022). This implies that the accumulation of MNC is controlled by the accessibility of decomposers rather than by carbon input in humid regions of alpine grasslands.

Conclusions

Based on a large-scale survey covering 3500 km, this study highlights the complex interplay between edaphic factors, climatic conditions, and vegetation characteristics in controlling MNC in alpine grasslands on the Tibetan Plateau. The significant variation in MNC content with changing climate zones emphasizes the importance of aridity for MNC reserves. A critical threshold of aridity (0.60) was observed that distinctly delineated the MNC response; MNC declined significantly below this threshold and plateaued beyond it. Moreover, aridity-dependent differences were observed in the drivers of MNC abundance between low and high aridity levels. Fungal necromass carbon represents the predominant fraction of MNC, especially under less arid conditions, and contributes to the long-term stability of SOC. Additionally, the contribution of species richness to MNC accrual was accentuated in the moisture-rich biomes of the Tibetan Plateau. These insights accentuate the cardinality of moisture for MNC modulation under distinct climatic

conditions, advocating for targeted management strategies to maintain MNC.

Data availability Data will be made available on request.

Declarations

Competing interest The authors state that there are no conflicts of interest.

References

Angst G, Mueller KE, Nierop KG, Simpson MJ (2021) Plant-or microbial-derived? A review on the molecular composition of stabilized soil organic matter. Soil Biol Biochem 156:108189. https://doi.org/10.1016/j.soilbio.2021.108189

Appuhn A, Joergensen RG (2006) Microbial colonisation of roots as a function of plant species. Soil Biol Biochem 38:1040–1051. https://doi.org/10.1016/j.soilbio.2005.09.002

Aran D, Maul A, Masfaraud J-F (2008) A spectrophotometric measurement of soil cation exchange capacity based on cobaltihexamine chloride absorbance. Cr Geosci 340:865–871. https://doi.org/10.1016/j.crte.2008.07.015

Bahram M, Hildebrand F, Forslund SK, Anderson JL, Soudzilovskaia NA, Bodegom PM, Bengtsson-Palme J, Anslan S, Coelho LP, Harend H (2018) Structure and function of the global topsoil microbiome. Nature 560:233–237. https://doi.org/10.1038/s41586-018-0386-6

Bai Y, Cotrufo MF (2022) Grassland soil carbon sequestration: Current understanding, challenges, and solutions. Science 377:603–608. https://doi.org/10.1126/science.abo2380

Bao Y, Bolan NS, Lai J, Wang Y, Jin X, Kirkham M, Wu X, Fang Z, Zhang Y, Wang H (2022) Interactions between organic matter and Fe (hydr) oxides and their influences on immobilization and remobilization of metal (loid) s: a review. Crit Rev Environ Sci Technol 52:4016–4037. https://doi.org/10.1080/10643389.2021.1974766

Berdugo M, Delgado-Baquerizo M, Soliveres S, Hernández-Clemente R, Zhao Y, Gaitán JJ, Gross N, Saiz H, Maire V, Lehmann A (2020) Global ecosystem thresholds driven by aridity. Science 367:787–790. https://doi.org/10.1126/science.aay5958

Cao Y, Ding J, Li J, Xin Z, Ren S, Wang T (2023) Necromass-derived soil organic carbon and its drivers at the global scale. Soil Biol Biochem 181:109025. https://doi.org/10.1016/j.soilbio.2023.109025

Chen G, Ma S, Tian D, Xiao W, Jiang L, Xing A, Zou A, Zhou L, Shen H, Zheng C (2020) Patterns and determinants of soil microbial residues from tropical to boreal forests. Soil Biol Biochem 151:108059. https://doi.org/10.1016/j.soilbio.2020.108059

Chen X, Hu Y, Xia Y, Zheng S, Ma C, Rui Y, He H, Huang D, Zhang Z, Ge T (2021) Contrasting pathways of carbon sequestration in

paddy and upland soils. Glob Change Biol 27:2478–2490. https://doi.org/10.1111/gcb.15595

Craig ME, Geyer KM, Beidler KV, Brzostek ER, Frey SD, Stuart Grandy A, Liang C, Phillips RP (2022) Fast-decaying plant litter enhances soil carbon in temperate forests but not through microbial physiological traits. Nat Commun 13:1229. https://doi.org/10.1038/s41467-022-28715-9

Deveau A, Bonito G, Uehling J, Paoletti M, Becker M, Bindschedler S, Hacquard S, Herve V, Labbe J, Lastovetsky OA (2018) Bacterial–fungal interactions: ecology, mechanisms and challenges. FEMS Microbiol Rev 42:335–352. https://doi.org/10.1093/femsre/fuy008

Ding X, Chen S, Zhang B, Liang C, He H, Horwath WR (2019) Warming increases microbial residue contribution to soil organic carbon in an alpine meadow. Soil Biol Biochem 135:13–19. https://doi.org/10.1016/j.soilbio.2019.04.004

Elith J, Leathwick JR, Hastie T (2008) A working guide to boosted regression trees. J Anim Ecol 77:802–813. https://doi.org/10.1111/j.1365-2656.2008.01390.x

Engelking B, Flessa H, Joergensen RG (2007) Shifts in amino sugar and ergosterol contents after addition of sucrose and cellulose to soil. Soil Biol Biochem 39:2111–2118. https://doi.org/10.1016/j.soilbio.2007.03.020

Friedlingstein P, O'Sullivan M, Jones MW, Andrew RM, Gregor L, Hauck J, Le Quéré C, Luijkx IT, Olsen A, Peters GP (2022) Global carbon budget 2022. Earth Syst Sci Data 2022:1–159. https://doi.org/10.5194/essd-14-4811-2022

Grace JB (2006) Structural equation modeling and natural systems. Cambridge University Press, Cambridge

Grace JB, Anderson TM, Seabloom EW, Borer ET, Adler PB, Harpole WS, Hautier Y, Hillebrand H, Lind EM, Pärtel M (2016) Integrative modelling reveals mechanisms linking productivity and plant species richness. Nature 529:390–393. https://doi.org/10.1038/nature16524

Hao Z, Zhao Y, Wang X, Wu J, Jiang S, Xiao J, Wang K, Zhou X, Liu H, Li J (2021) Thresholds in aridity and soil carbon-to-nitrogen ratio govern the accumulation of soil microbial residues. Commun Earth Environ 2:236. https://doi.org/10.1038/s43247-021-00306-4

He L, Rodrigues JLM, Soudzilovskaia NA, Barceló M, Olsson PA, Song C, Tedersoo L, Yuan F, Yuan F, Lipson DA (2020) Global biogeography of fungal and bacterial biomass carbon in topsoil. Soil Biol Biochem 151:108024. https://doi.org/10.1016/j.soilbio.2020.108024

He M, Fang K, Chen L, Feng X, Qin S, Kou D, He H, Liang C, Yang Y (2022) Depth-dependent drivers of soil microbial necromass carbon across Tibetan alpine grasslands. Glob Change Biol 28:936–949. https://doi.org/10.1111/gcb.15969

Heckman KA, Possinger AR, Badgley BD, Bowman MM, Gallo AC, Hatten JA, Nave LE, SanClements MD, Swanston CW, Weiglein TL (2023) Moisture-driven divergence in mineral-associated soil carbon persistence. P Natl Acad Sci USA 120:e2210044120. https://doi.org/10.1073/pnas.2210044120

Hicks Pries CE, Castanha C, Porras R, Torn M (2017) The whole-soil carbon flux in response to warming. Science 355:1420–1423. https://doi.org/10.1126/science.aal131

Hu Y, Zheng Q, Noll L, Zhang S, Wanek W (2020) Direct measurement of the in situ decomposition of microbial-derived soil organic matter. Soil Biol Biochem 141:107660. https://doi.org/10.1016/j.soilbio.2019.107660

Huang H, Calabrese S, Rodriguez-Iturbe I (2021) Variability of ecosystem carbon source from microbial respiration is controlled by rainfall dynamics. P Natl Acad Sci USA 118:e2115283118. https://doi.org/10.1073/pnas.2115283118

Jeewani PH, Luo Y, Yu G, Fu Y, He X, Van Zwieten L, Liang C, Kumar A, He Y, Kuzyakov Y (2021) Arbuscular mycorrhizal fungi and goethite promote carbon sequestration via hyphal-aggregate

mineral interactions. Soil Biol Biochem 162:108417. https://doi.org/10.1016/j.soilbio.2021.108417

Jia Y, Zhai G, Zhu S, Liu X, Schmid B, Wang Z, Ma K, Feng X (2021) Plant and microbial pathways driving plant diversity effects on soil carbon accumulation in subtropical forest. Soil Biol Biochem 161:108375. https://doi.org/10.1016/j.soilbio.2021.108375

Joergensen RG (2018) Amino sugars as specific indices for fungal and bacterial residues in soil. Biol Fert Soils 54:559–568. https://doi.org/10.1007/s00374-018-1288-3

Koester M, Stock SC, Nájera F, Abdallah K, Gorbushina A, Prietzel J, Matus F, Klysubun W, Boy J, Kuzyakov Y (2021) From rock eating to vegetarian ecosystems—disentangling processes of phosphorus acquisition across biomes. Geoderma 388:114827. https://doi.org/10.1016/j.geoderma.2020.114827

Kramer MG, Chadwick OA (2018) Climate-driven thresholds in reactive mineral retention of soil carbon at the global scale. Nat Clim Change 8:1104–1108. https://doi.org/10.1038/s41558-018-0341-4

Lai J, Zou Y, Zhang J, Peres-Neto PR (2022) Generalizing hierarchical and variation partitioning in multiple regression and canonical analyses using the rdacca. hp R package. Methods Ecol Evol 13:782–788. https://doi.org/10.1111/2041-210x.13800

Lalonde K, Mucci A, Ouellet A, Gélinas Y (2012) Preservation of organic matter in sediments promoted by iron. Nature 483:198–200. https://doi.org/10.1038/nature10855

Lange M, Eisenhauer N, Sierra CA, Bessler H, Engels C, Griffiths RI, Mellado-Vázquez PG, Malik AA, Roy J, Scheu S (2015) Plant diversity increases soil microbial activity and soil carbon storage. Nat Commun 6:6707. https://doi.org/10.1038/ncomms7707

Li X, Huang J, Qu C, Chen W, Chen C, Cai P, Huang Q (2022) Diverse regulations on the accumulation of fungal and bacterial necromass in cropland soils. Geoderma 410:115675. https://doi.org/10.1016/j.geoderma.2021.115675

Li Y, Xiao M, Wei L, Liu Q, Zhu Z, Yuan H, Wu J, Yuan J, Wu X, Kuzyakov Y, Ge T (2024) Bacterial necromass determines the response of mineral-associated organic matter to elevated CO_2. Biol Fert Soils 60:327–340. https://doi.org/10.1007/s00374-024-01803-2

Liang C, Schimel JP, Jastrow JD (2017) The importance of anabolism in microbial control over soil carbon storage. Nat Microbiol 2:1–6. https://doi.org/10.1038/nmicrobiol.2017.105

Liang C, Amelung W, Lehmann J, Kästner M (2019) Quantitative assessment of microbial necromass contribution to soil organic matter. Glob Change Biol 25:3578–3590. https://doi.org/10.1111/gcb.14781

Liu Y, Zou X, Chen HY, Delgado-Baquerizo M, Wang C, Zhang C, Ruan H (2023) Fungal necromass is reduced by intensive drought in subsoil but not in topsoil. Glob Change Biol 29:7159–7172. https://doi.org/10.1111/gcb.16978

Lu R (1999) Analysis methods of soil agricultural chemistry. China Agricultural Science and Technology Press, Beijing, China

Luo Y, Xiao M, Yuan H, Liang C, Zhu Z, Xu J, Kuzyakov Y, Wu J, Ge T, Tang C (2021) Rice rhizodeposition promotes the build-up of organic carbon in soil via fungal necromass. Soil Biol Biochem 160:108345. https://doi.org/10.1016/j.soilbio.2021.108345

Ma T, Zhu S, Wang Z, Chen D, Dai G, Feng B, Su X, Hu H, Li K, Han W (2018) Divergent accumulation of microbial necromass and plant lignin components in grassland soils. Nat Commun 9:3480. https://doi.org/10.1038/s41467-018-05891-1

Ma S, Zhu B, Chen G, Ni X, Zhou L, Su H, Cai Q, Chen X, Zhu J, Ji C (2022) Loss of soil microbial residue carbon by converting a tropical forest to tea plantation. Sci Total Environ 818:151742. https://doi.org/10.1016/j.scitotenv.2021.151742

Mellado-Vázquez PG, Lange M, Bachmann D, Gockele A, Karlowsky S, Milcu A, Piel C, Roscher C, Roy J, Gleixner G (2016) Plant diversity generates enhanced soil microbial access to recently

photosynthesized carbon in the rhizosphere. Soil Biol Biochem 94:122–132. https://doi.org/10.1016/j.soilbio.2015.11.012

Prommer J, Walker TW, Wanek W, Braun J, Zezula D, Hu Y, Hofhansl F, Richter A (2020) Increased microbial growth, biomass, and turnover drive soil organic carbon accumulation at higher plant diversity. Glob Change Biol 26:669–681. https://doi.org/10.1111/gcb.14777

Qu Q, Deng L, Gunina A, Hai X, Deng J, Shangguan Z, Kuzyakov Y (2024) Grazing exclusion increases soil organic C through microbial necromass of root-derived C as traced by ^{13}C labelling photosynthate. Biol Fert Soils 60:407–420. https://doi.org/10.1007/s00374-024-01807-y

R Core Team (2023) R: a language and environment for statistical computing. R Foundation for Statistical Computing. Vienna, Austria. https://www.R-project.org

Rasmussen C, Heckman K, Wieder WR, Keiluweit M, Lawrence CR, Berhe AA, Blankinship JC, Crow SE, Druhan JL, Hicks Pries CE, Marin-Spiotta E, Plante AF, Schädel C, Schimel JP, Sierra CA, Thompson A, Wagai R (2018) Beyond clay: towards an improved set of variables for predicting soil organic matter content. Biogeochemistry 137:297–306. https://doi.org/10.1007/s10533-018-0424-3

Rousk J, Brookes PC, Bååth E (2009) Contrasting Soil pH Effects on Fungal and Bacterial Growth Suggest Functional Redundancy in Carbon Mineralization. Appl Environ Microb 75:1589–1596. https://doi.org/10.1128/Aem.02775-08

Shao P, He H, Zhang X, Xie H, Bao X, Liang C (2018) Responses of microbial residues to simulated climate change in a semiarid grassland. Sci Total Environ 644:1286–1291. https://doi.org/10.1016/j.scitotenv.2018.07.055

Shipley B (2016) Cause and correlation in biology: a user's guide to path analysis, structural equations and causal inference with R. Cambridge University Press, Cambridge, UK

Six J, Frey S, Thiet R, Batten K (2006) Bacterial and fungal contributions to carbon sequestration in agroecosystems. Soil Sci Soc Am J 70:555–569. https://doi.org/10.2136/sssaj2004.0347

Slessarev E, Lin Y, Bingham N, Johnson J, Dai Y, Schimel J, Chadwick O (2016) Water balance creates a threshold in soil pH at the global scale. Nature 540:567–569. https://doi.org/10.1038/nature20139

Sokol NW, Slessarev E, Marschmann GL, Nicolas A, Blazewicz SJ, Brodie EL, Firestone MK, Foley MM, Hestrin R, Hungate BA (2022) Life and death in the soil microbiome: how ecological processes influence biogeochemistry. Nat Rev Microbiol 20:415–430. https://doi.org/10.1038/s41579-022-00695-z

Spohn M, Bagchi S, Biederman LA, Borer ET, Bråthen KA, Bugalho MN, Caldeira MC, Catford JA, Collins SL, Eisenhauer N (2023) The positive effect of plant diversity on soil carbon depends on climate. Nat Commun 14:6624. https://doi.org/10.1038/s41467-023-42340-0

Terrer C, Phillips RP, Hungate BA, Rosende J, Pett-Ridge J, Craig ME, van Groenigen KJ, Keenan TF, Sulman BN, Stocker BD (2021) A trade-off between plant and soil carbon storage under elevated CO_2. Nature 591:599–603. https://doi.org/10.1038/s41586-021-03306-8

UNEP (United Nations Environment Programme) (2022) A scientific assessment of the third pole environment. Nairobi, Kenya. https://www.unep.org/resources/report/scientific-assessment-third-pole-environment

Veloso M, Angers D, Chantigny M, Bayer C (2020) Carbon accumulation and aggregation are mediated by fungi in a subtropical soil under conservation agriculture. Geoderma 363:114159. https://doi.org/10.1016/j.geoderma.2019.114159

Wagai R, Kajiura M, Asano M (2020) Iron and aluminum association with microbially processed organic matter via meso-density aggregate formation across soils: organo-metallic glue hypothesis. Soil 2020:1–42. https://doi.org/10.5194/soil-6-597-2020

Wang B, An S, Liang C, Liu Y, Kuzyakov Y (2021a) Microbial necromass as the source of soil organic carbon in global ecosystems. Soil Biol Biochem 162:108422. https://doi.org/10.1016/j.soilbio.2021.108422

Wang C, Qu L, Yang L, Liu D, Morrissey E, Miao R, Liu Z, Wang Q, Fang Y, Bai E (2021b) Large-scale importance of microbial carbon use efficiency and necromass to soil organic carbon. Glob Change Biol 27:2039–2048. https://doi.org/10.1111/gcb.15550

Wen S, Chen J, Yang Z, Deng L, Feng J, Zhang W, Zeng XM, Huang Q, Delgado-Baquerizo M, Liu YR (2023) Climatic seasonality challenges the stability of microbial-driven deep soil carbon accumulation across China. Glob Change Biol. https://doi.org/10.1111/gcb.16760

Whalen ED, Grandy AS, Sokol NW, Keiluweit M, Ernakovich J, Smith RG, Frey SD (2022) Clarifying the evidence for microbial- and plant-derived soil organic matter, and the path toward a more quantitative understanding. Glob Change Biol 28:7167–7185. https://doi.org/10.1111/gcb.16413

White RP, Murray S, Rohweder M, Prince S, Thompson K (2000) Pilot analysis of global ecosystems: grassland ecosystems. World Resources Institute, Washington, DC

Wiesmeier M, Urbanski L, Hobley E, Lang B, von Lützow M, Marin-Spiotta E, van Wesemael B, Rabot E, Ließ M, Garcia-Franco N (2019) Soil organic carbon storage as a key function of soils- A review of drivers and indicators at various scales. Geoderma 333:149–162. https://doi.org/10.1016/j.geoderma.2018.07.026

Xia Y, Chen X, Hu Y, Zheng S, Ning Z, Guggenberger G, He H, Wu J, Su Y (2019) Contrasting contribution of fungal and bacterial residues to organic carbon accumulation in paddy soils across eastern China. Biol Fert Soils 55:767–776. https://doi.org/10.1007/s00374-019-01390-7

Xiao K-Q, Zhao Y, Liang C, Zhao M, Moore OW, Otero-Fariña A, Zhu Y-G, Johnson K, Peacock CL (2023) Introducing the soil mineral carbon pump. Nat Rev Earth Environ 4:135–136. https://doi.org/10.1038/s43017-023-00396-y

Xu S, Geng W, Sayer EJ, Zhou G, Zhou P, Liu C (2020) Soil microbial biomass and community responses to experimental precipitation change: A meta-analysis. Soil Ecol Lett 2:93–103. https://doi.org/10.1007/s42832-020-0033-7

Xu Y, Gao X, Pei J, Sun L, Wang J (2022) Crop root vs. shoot incorporation drives microbial residue carbon accumulation in soil aggregate fractions. Biol Fert Soils 58:843–854. https://doi.org/10.1007/s00374-022-01666-5

Xue Y, Liu W, Feng Q, Zhu M, Wang L, Chen Z, Zhang J (2023) Variations and controls of soil microbial necromass carbon in grasslands along aridity gradients. Ecol Indic 156:111188. https://doi.org/10.1016/j.ecolind.2023.111188

Yang Y, Xie H, Mao Z, Bao X, He H, Zhang X, Liang C (2022) Fungi determine increased soil organic carbon more than bacteria through their necromass inputs in conservation tillage croplands. Soil Biol Biochem 167:108587. https://doi.org/10.1016/j.soilbio.2022.108587

Zhang X, Amelung W (1996) Gas chromatographic determination of muramic acid, glucosamine, mannosamine, and galactosamine in soils. Soil Biol Biochem 28:1201–1206. https://doi.org/10.1016/0038-0717(96)00117-4

Zhang X, Jia J, Chen L, Chu H, He J-S, Zhang Y, Feng X (2021) Aridity and NPP constrain contribution of microbial necromass to soil organic carbon in the Qinghai-Tibet alpine grasslands. Soil Biol Biochem 156:108213. https://doi.org/10.1016/j.soilbio.2021.108213

Zhang J, Feng Y, Maestre FT, Berdugo M, Wang J, Coleine C, Sáez-Sandino T, García-Velázquez L, Singh BK, Delgado-Baquerizo M (2023) Water availability creates global thresholds in

multidimensional soil biodiversity and functions. Nat Ecol Evol 7:1–10. https://doi.org/10.1038/s41559-023-02071-3

Zhao Y, Wang X, Jiang S, Zhou XH, Liu H, Xiao J, Hao Z, Wang K (2021) Climate and geochemistry interactions at different altitudes influence soil organic carbon turnover times in alpine grasslands. Agr Ecosyst Environ 320:107591. https://doi.org/10.1016/j.agee.2021.107591

Zhao Y, Wang X, Jiang S, Xiao J, Li J, Zhou X, Liu H, Hao Z, Wang K (2022) Soil development mediates precipitation control on plant productivity and diversity in alpine grasslands. Geoderma 412:115721. https://doi.org/10.1016/j.geoderma.2022.115721

Zhao Y, Wang X, Chen F, Li J, Wu J, Sun Y, Zhang Y, Deng T, Jiang S, Zhou X (2023) Soil organic matter enhances aboveground biomass in alpine grassland under drought. Geoderma 433:116430. https://doi.org/10.1016/j.geoderma.2023.116430